Polymer Journal (2016) 48, 1039–1044

www.nature.com/pj

FOCUS REVIEW

Structures of silk fibroin before and after spinning and biomedical applications

Yu Suzuki

Silkworms produce silk fibroin fibers from an aqueous silk fibroin solution by applying shear stress within the spinneret at ambient temperature. This process is an attractive model for developing sustainable fiber processing technology. However, to completely elucidate the fibroin processing mechanism, the structures of fibroin before and after spinning need to be determined. In this study, we report the structures of silk fibroin before and after spinning, determined by solution and solid-state nuclear magnetic resonance (NMR). The pre-spinning structure of fibroin tandem repeat sequences was determined by solution NMR, using native liquid silk extracted from silkworm larvae. In addition, the precise lamellar structure of fibroin after spinning was investigated through a combination of stable isotope labeling of model peptides and solid-state NMR. Moreover, a silk-based small diameter vascular graft was developed by electrospinning and was subsequently evaluated *in vivo*. These studies may provide a perspective for investigation of energy-conserving fiber processing techniques and silk-based biomedical materials.
Polymer Journal (2016) **48,** 1039–1044; doi:10.1038/pj.2016.77; published online 7 September 2016

INTRODUCTION

Silk fibroin fibers produced from the silk of the mulberry silkworm *Bombyx mori* has outstanding mechanical properties, including high strength and toughness, despite being spun from an aqueous solution at ambient temperature. A fibroin molecule consists of a heavy chain of 391 kDa and a light chain of 26 kDa connected by a disulfide bond.[1–4] The primary structure of *B. mori* fibroin has an unusual repeat sequence in the heavy chain, as shown in Figure 1. This structure comprises a highly repetitive Gly-Ala-Gly-Ala-Gly-Ser (GAGAGS) sequence, relatively fewer repetitive sequences of hydrophobic and/or aromatic residues and amorphous regions containing negatively charged, polar, bulky hydrophobic and/or aromatic residues.

Silk proteins are secreted and stored in silk glands before they are processed into fibers. Silkworms produce fibroin fibers from an aqueous fibroin solution by applying shear stress within the spinneret and applying tension, which is induced by the repeated drawing back of the silkworm's head, at ambient temperature. As such, silk fiber processing is an attractive model for developing sustainable fiber processing technology. However, a complete understanding of the fibroin processing mechanism requires the determination of fibroin structures before and after spinning.

Herein I report the structural nuclear magnetic resonance (NMR) analyses of fibroin before and after spinning. NMR is a suitable method to study the silk fibroin structure because it can determine the atomic-level molecular structure of various sample forms ranging from solutions to solids. In this study, fibroin stored in the middle silk gland, called 'liquid silk,' was characterized to determine the molecular structures before spinning into *B. mori* and *Samia cynthia ricini* (*S. c. ricini*) silks. Second, the precise structure of fibroin after spinning was determined using a combination of site-specific stable isotope-labeled peptides and solid-state NMR. Third, the fibroin structure in fluorinated solvents and the interaction between model peptides and solvent molecules were studied to determine the relation between the molecular structure and the physical properties of regenerated silk fibers. Finally, the development of silk-based small-diameter vascular grafts by electrospinning was demonstrated as an example of the application of silks as biomedical materials.

SOLUTION STRUCTURES OF REPEAT SEQUENCES IN *B. mori* LIQUID SILK

The structural features of *B. mori* fibroin can be conveniently studied by using the synthetic peptide $(AG)_n$ as a model for the crystalline region.[5,6] Through solid-state NMR, the backbone structure of $(AG)_n$ before spinning was determined to be a repeated type II β-turn structure. Next we determined the solution structure of fibroin molecules in native liquid silk extracted from *B. mori* silkworm larvae. The solution structure of native liquid silk, especially for tandem repeat sequences with $(GAGXGA)_n$ (X = Ser, Tyr or Val) and GAASGA motifs, was then determined by solution NMR.[7]

The sample preparation procedures for non-labeled and ^{13}C-labeled liquid silks were as follows: the silk glands containing liquid silk were extracted from *B. mori* larvae from the sixth to eighth days of the fifth instar and soaked in a container filled with distilled H_2O so that the liquid silk could be gently removed from the glands. The liquid silk was then soaked six times in freshly distilled H_2O for 5 min to remove sericin from the silk's surface.[8] Next the liquid silk was placed in a 5-mm-diameter NMR tube together with a sealed capillary containing

Tenure-Track Program for Innovative Research, University of Fukui, Fukui, Japan
Correspondence: Dr Y Suzuki, Tenure-Track Program for Innovative Research, University of Fukui, 3-9-1 Bunkyo, Fukui-shi, Fukui 910-8507, Japan.
E-mail: suzukiyu@u-fukui.ac.jp
Received 7 February 2016; revised 13 June 2016; accepted 4 July 2016; published online 7 September 2016

D_2O for NMR locking. Uniformly ^{13}C-labeled liquid silk from *B. mori* was biosynthetically prepared by feeding the silkworm larvae with U-^{13}C D-glucose added to their artificial diet. By comparing ^{13}C-^{13}C coupled peak intensities with corresponding ^{12}C-^{13}C non-coupled peak intensities for a given nucleus, the ^{13}C labeling was determined to be approximately 80%.

The ^{1}H-^{15}N heteronuclear single-quantum correlation spectrum of natural abundant liquid silk is shown in Figure 2a; it exhibits relatively sharp and fairly well-separated cross peaks despite the very high molecular weight of fibroin. The ^{1}H, ^{15}N and ^{13}C resonances for residues in the repetitive motifs GAGXGAG (X = S, Y or V) and GAASGA were assigned by multidimensional NMR analyses. The results of the chemical shifts for Ala $^{13}C\alpha$ and $^{13}C\beta$ indicated that these motifs have neither typical α-helix nor β-sheet structures.[9,10]

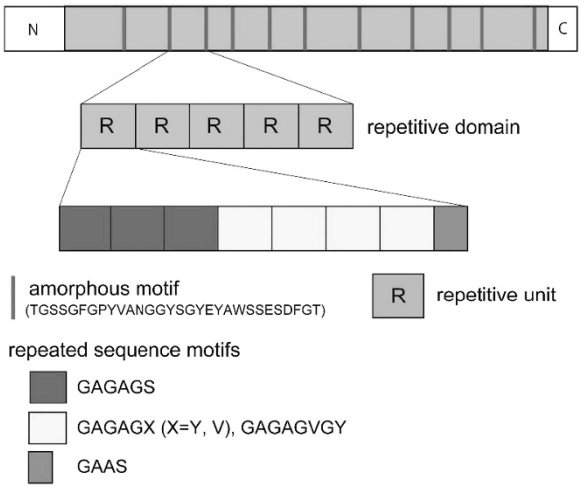

Figure 1 Schematic of the organization of 12 repetitive domains and 11 amorphous repeat motifs in the *B. mori* silk fibroin heavy chain primary structure. The repetitive domains comprise 1–8 repeats of repetitive unit R, which consists of three repeated elements of sequence motifs. A full color version of this figure is available at the *Polymer Journal* online.

The peaks of liquid silk were relatively broad because of the very condensed (approximately 25% w/v) sample solution, and they overlapped because of tandem repeat sequences. Therefore, the standard three-dimensional structure determination technique based on the distance geometry method was not applicable. The TALOS-N[11] program is a database system used for the empirical prediction of backbone torsion angles (ϕ, ψ) through a combination of six types of backbone chemical shifts ($^{1}H\alpha$, $^{13}C\alpha$, $^{13}C\beta$, ^{13}CO, ^{15}N and ^{1}HN) and sequence information. This program was used to obtain structural information about the four motifs. Figure 2b shows the (ϕ, ψ) database for (i+1) and (i+2) residues in typical β-turn structures formed with four amino acids ($i-i$+3) for five types of β-turns in well-defined crystal structures.[12] Figure 2c shows the (ϕ, ψ) maps of the 25 closest database matches predicted for the four motifs. As evident in Figure 2c, the 25 database heptapeptides matched to the target motif GAGXGAG (X = S, Y or V) show that the torsion angles of the residues (A^2, X^4 and A^6) fall into narrow regions of the (i+1) residue in typical type II β-turn structures. In contrast, the Gly residues (G^3, G^5 and G^7) fall into regions of the (i+2) residue in typical type II β-turn structures as well as other regions. Notably, for the G^5 residues in the GAGYGAG and GAGVGAG motifs, a larger number of the matches of torsion angles outside the regions of typical type II β-turn structures were predicted by TALOS-N than for the corresponding G^5 residue in the GAGSGAG motif. This observation suggests that the repeated type II β-turn structures for the former two motifs are less stable than the latter GAGSGAG motif.

In contrast to the three aforementioned motifs, the predicted (ϕ, ψ) for residues A^3S^4 in the GAASGA motif were scattered and inconsistent with the (ϕ, ψ) maps for any typical secondary structure, thus indicating that the motif assumes a random-coil structure. A replacement of Gly by Ala at the third position in the $G^1A^2G^3S^4G^5A^6$ motif destabilizes the type II β-turn structure because a Gly residue without

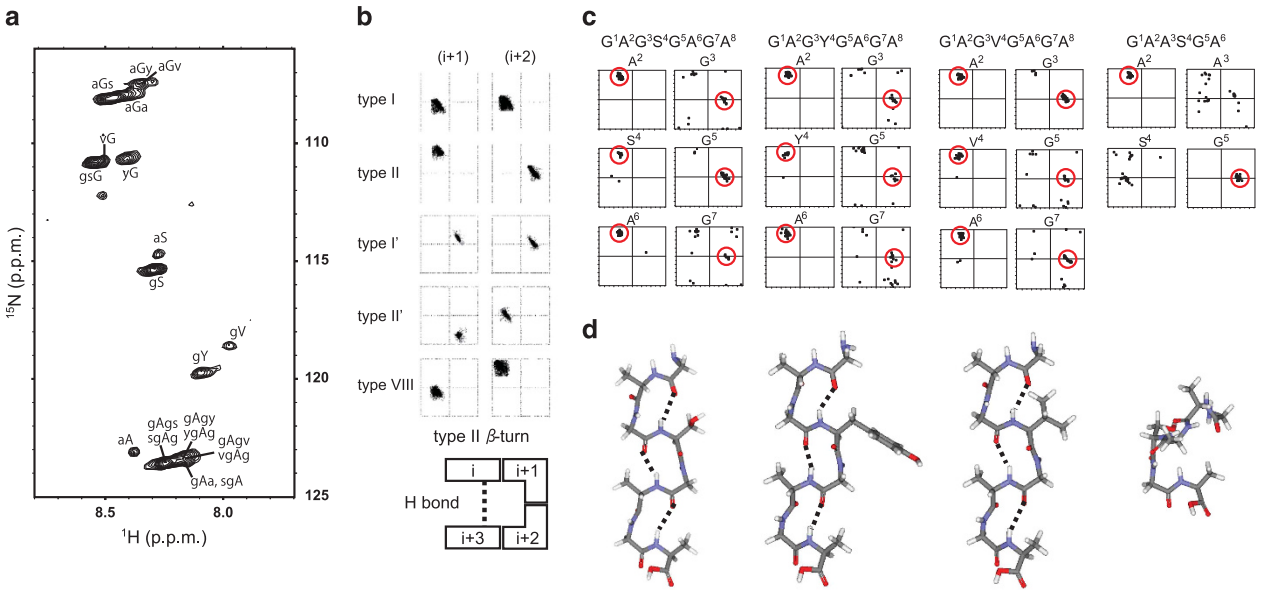

Figure 2 (**a**) ^{1}H-^{15}N HSQC spectrum and peak assignments of natural abundant *B. mori* liquid silk. Peak assignments represent amide protons and nitrogen resonances of corresponding residues (upper case) and neighboring residues (lower case); (**b**) (ϕ, ψ) maps for typical type I, type II, type I′, type II′ and type VIII β-turns from the literature[12] and an illustration of the type II β-turn conformation; (**c**) 25 best matches for torsion angles (ϕ, ψ) for GAGXGAG (X = S, Y or V) and GAASG motifs obtained using the TALOS-N program; and (**d**) structural models constructed using averaged (ϕ, ψ) (in the red circle) for each motif. Hydrogen bonds are assumed to exist between the HN of the i-th and CO of the (i+3)th residues for GAGXGAG (X = S, Y or V) motifs.

a bulky side chain is favored at this position with a positive (left-handed) ϕ value in the β-turn, whereas a positive value of ϕ is energetically unfavorable for Ala. Figure 2d shows structural models constructed using average torsion angles for the 25 best matches (ϕ, ψ) for each motif. The models for GAGXGAG (X = S, Y or V) show hydrogen bond formation between the HN of the *i*-th and CO of the (*i*+3)th residues, which characterizes the β-turn structure. Furthermore, inter-residue HN-Hα nuclear Overhauser effect (NOE) cross peaks between the *i*-th and (*i*+2)th residues in GAGXGA (X = S, Y or V) motifs were observed, supporting the repeated type II β-turn structure. Thus the presence of a repeated type II β-turn structure in *B. mori* liquid silk was identified.

SOLUTION STRUCTURES OF REPEAT SEQUENCES IN *S. c. ricini* LIQUID SILK

In addition to *B. mori*, various wild silkworms produce fibroin with a unique primary and higher-order structure. Recently, silk from these wild silkworms has received attention as a potentially valuable material.[13–15] The diverse mechanical properties and morphologies of various wild silks are advantageous for developing novel biomaterials with appropriate properties for specific applications. *S. c. ricini* is one such wild silkworm and the primary structure of its fibroin consists of tandem repeat sequences composed of polyalanine and Gly-rich regions.[16] The primary structure of fibroin from *S. c. ricini* resembles that of spider dragline silk.[17–19] The fibroin structure of *S. c. ricini* before spinning was examined in the same manner as that of *B. mori*.

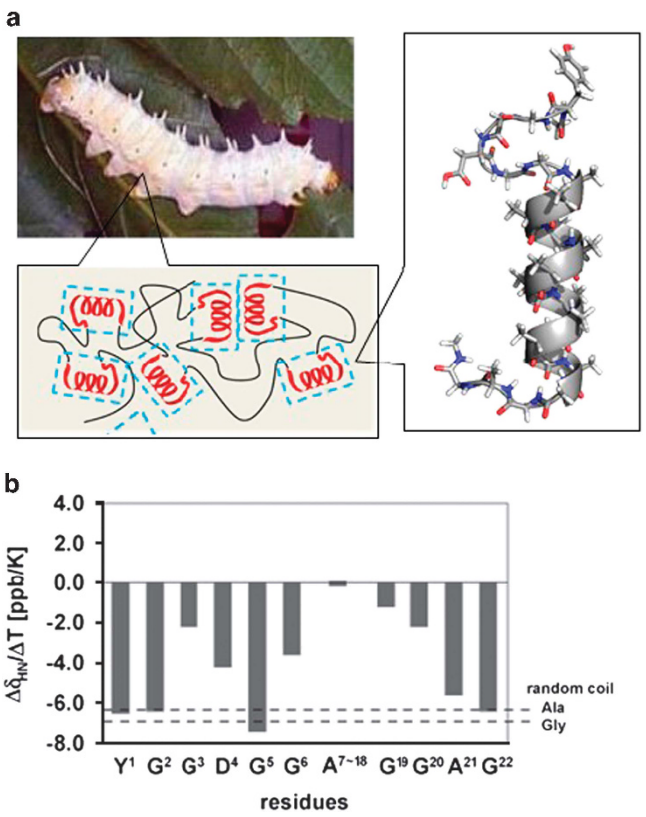

Figure 3 (**a**) An *S. c. ricini* larva, a depiction of the fibroin molecule in a silk gland and an energy-minimized model structure of YGGDGG(A)$_{12}$GGAG constructed from estimates of backbone dihedral angles using the TALOS-N program; and (**b**) a plot of amide proton temperature coefficients for the *S. c. ricini* repeat motif in liquid silk with those of Ala and Gly in *B. mori* as random-coil references (shown as dashed lines).

A sequential assignment of the most common *S. c. ricini* fibroin repeat motif Y^{1}GGDGG^{6}(A)$_{12}$G^{19}GAG^{22} was determined by solution NMR for liquid silk extracted from *S. c. ricini* larvae. Using the ^{1}H, ^{13}C and ^{15}N chemical shifts and TALOS-N, we developed a model consisting of a typical α-helix structure for the polyalanine region and capping structures for terminal regions (Figure 3a). In addition, we analyzed amide proton temperature coefficients to verify the structure. A change in the amide proton chemical shift as a function of temperature can be used as an indicator of hydrogen bond formation. In general, the coefficients of backbone amide protons in a random coil configuration are rather large and negative (that is, < -6.5 p.p.b. K^{-1}). Examination of amide temperature coefficients strongly suggested that the polyalanine region forms an α-helix (Figure 3b). Moreover, N- and C-terminal regions form capping motifs, which adopt a Schellman C-cap structure at the C terminus. The terminal cap motifs stabilize the polyalanine α-helix. Capping motifs may have a role in preventing both the structural transition from α-helix to β-sheet and fibril formation inside the silkworm body, which would be fatal to the silkworm.[20]

STRUCTURE OF THE CRYSTALLINE DOMAIN OF *B. mori* SILK FIBROIN

The fibroin structure after spinning was first proposed to be an antiparallel β-sheet structure by Marsh *et al.*[21] on the basis of a fiber diffraction study of native *B. mori* silk fiber. Later, Fraser *et al.*,[22] Lotz *et al.*[23] and Takahashi *et al.*[24] reported some intrinsic structural disorders in this antiparallel β-sheet model of fibroin. Moreover, the Ala Cβ peak in the solid-state NMR spectrum of [3-^{13}C]Ala *B. mori* silk fiber is broad and asymmetric, reflecting the heterogeneous structure of silk fiber.[25,26] Conformation-dependent NMR chemical shifts can be used to easily and selectively determine the fraction of mixed structures. Furthermore, the atomic-level structure can be obtained by using NMR with a stable isotope labeling of model peptides. The sequential peptide model of the crystalline region (AGSGAG)$_5$ was evaluated by solid-state NMR.[27,28]

The fractions of random-coil and/or distorted β-turn components of each Ala residue were determined by using ^{13}C CP/MAS NMR spectra of versions of [3-^{13}C]Ala-(AGSGAG)$_5$ with 10 different ^{13}C labeling positions. In addition, the fractions of random-coil and/or distorted β-turn components of each Ser residue were determined from the ^{13}C-^{15}N atomic distances of five versions of the peptide with different [1-^{13}C]Gly-Ser-[^{15}N]Gly positions evaluated by rotational-echo double-resonance experiments. In this manner, the fractions of distorted β-turn and/or random-coil components were determined. Figure 4a shows that these data plotted against the residue position within (AGSGAG)$_5$; the result suggests the appearance of a folded lamellar structure with two β-turns, one at approximately residue 11 and the other at approximately residue 19. By combining the structural information of Ala and Ser residues from solid-state NMR and statistical mechanical calculations, we proposed probable lamellar structures of (AGSGAG)$_5$ with two turns at the central part of the sequence consisting of 8–12 amino acids (Figure 4b).

INTERACTIONS BETWEEN FIBROIN AND FLUORINATED ALCOHOLS FOR PREPARATION OF REGENERATED SILK FIBER

Fibroin has been developed into a wide range of forms such as microparticles, films, foams, sponges and composites.[29] The

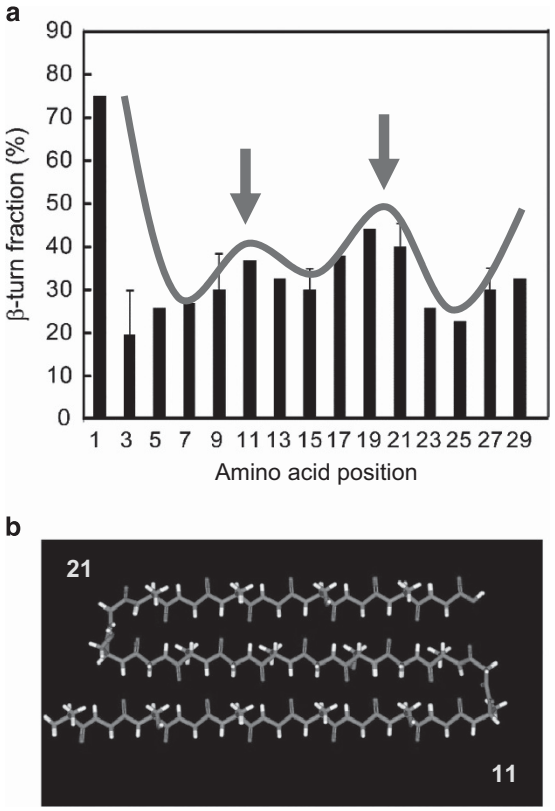

Figure 4 (**a**) Observed relative intensities of the distorted β-turn component of $(AGSGAG)_5$ obtained from the peak at 16.7 p.p.m. of Ala Cβ and REDOR bimodal fitting for Ser residues shown for different positions; and (**b**) a probable lamellar structure and turn-placed residue number of $(AGSGAG)_5$ obtained by combining solid-state NMR and statistical mechanical calculations. A full color version of this figure is available at the *Polymer Journal* online.

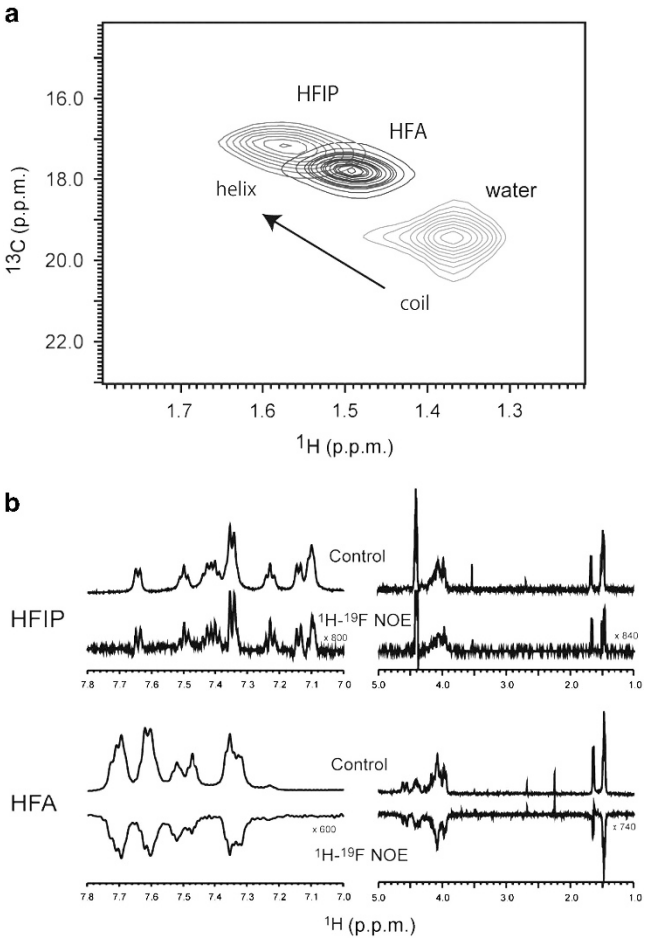

Figure 5 (**a**) Overlaid ^{1}H-^{13}C HSQC spectra of the Ala methyl region for fibroin in HFIP, HFA and water; and (**b**) ^{1}H-^{19}F intermolecular NOE spectra of $(AGSGAG)_2$ in HFIP and HFA. The upper spectra are the observed 1D ^{1}H spectra (control) and the lower spectra are the ^{1}H-^{19}F NOE spectra. A full color version of this figure is available at the *Polymer Journal* online.

processing of such wide range of forms requires solvents that dissolve fibroin. The fluorinated organic solvents 1,1,1,3,3,3-hexafluoro-2-propanol (HFIP) and hexafluoroacetone trihydrate (HFA) have been successfully used to produce regenerated fibroin fibers with high strength.[30–33] To understand the reasons for the difference in strength between regenerated silk fibers prepared from these two solvents, we compared the properties of native fibroin and $(AGSGAG)_2$, a model for the crystalline part of fibroin, in the two solvents. The ^{13}C and ^{1}H chemical shifts obtained from ^{1}H-^{13}C heteronuclear single-quantum correlation spectra of fibroin in HFIP, HFA and water indicate that fibroin forms a helix-like structure in the fluorinated alcohols and a random-coil structure in water (Figure 5a). The intramolecular ^{1}H-^{1}H NOE data for $(AGSGAG)_2$ imply the presence of helical structures in the middle part of the peptide in HFIP but not in HFA. Moreover, ^{1}H-^{19}F NOE experiments indicate that peptide–solvent interactions in HFA persist longer than those in HFIP (Figure 5b).[34]

In processes that produce regenerated silk fibers from a silk solution, the solution typically travels through a spinneret into methanol to achieve coagulation. Coagulation involves the removal of solvents around dissolved fibroin, thereby producing a conformational transition of the crystalline regions of fibroin to β-sheet structures. Regenerated fibers prepared from HFIP solution with an appropriate draw ratio exhibit a tensile strength slightly greater than that of native silk fibers; however, the strength of regenerated fibers prepared from the HFA solution was approximately 40% less than that of native silk fiber.[35] The X-ray diffraction patterns indicate that this difference in the tensile strength of regenerated silk fibers between the two solvents arises from the difference in the long-range orientation of crystalline regions.[35] According to these results, the displacement of HFA molecules during coagulation may be less complete because of the relatively stronger interactions of HFA with fibroin molecules, as revealed by ^{1}H-^{19}F NOE experiments. A less extensive β-sheet aggregation during coagulation can occur, leading to a relatively lower tensile strength of fibers from HFA solutions. Furthermore, the silk model peptide conformation possesses a helical structure in HFIP compared with a loosed helical structure in HFA, which suggests that fibroin with more extensive helical conformations in HFIP tend to align more like a native silk solution in a silk gland and favor extensive β-sheet aggregation.

DEVELOPMENT OF SILK/POLYURETHANE SMALL-DIAMETER VASCULAR GRAFT BY ELECTROSPINNING

Silk fibroin fiber has a long history of use as a suture in surgery because of its biocompatibility and diverse mechanical properties. Currently, silk fibroin remains an attractive candidate for use as biomedical material. Fibroin has high strength and toughness but less

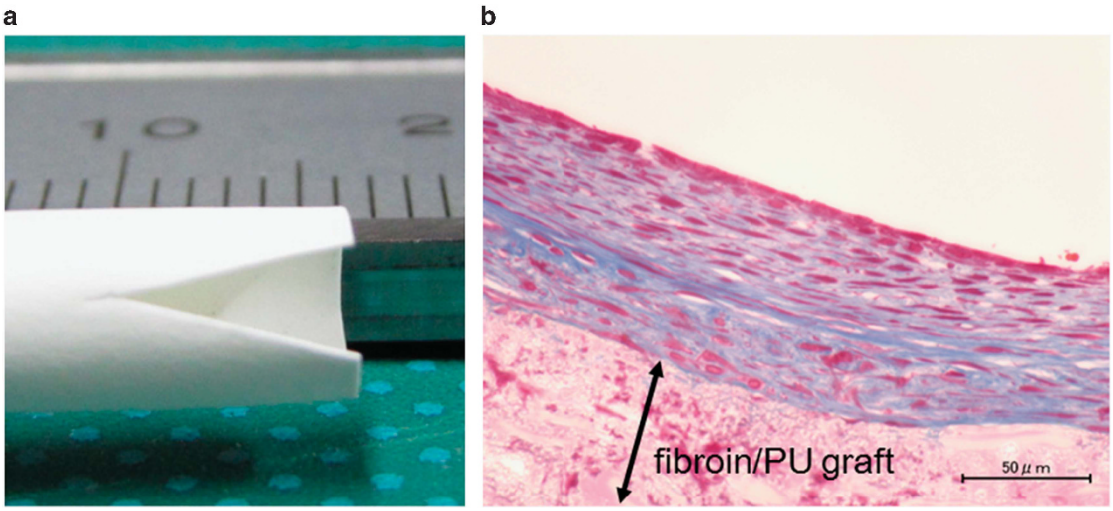

Figure 6 (**a**) A fibroin/polyurethane graft with an inner diameter of 3.5 mm. No fraying is observed at the cutting surfaces; and (**b**) histological MTC staining of the graft implanted into a rat for 2 weeks. The organization of the blood-vessel wall composed of collagen, smooth muscle cells and endothelial cells was observed on the inner side of the graft surface.

elasticity than collagen and elastin, which are components of the extracellular matrix. Appropriate elasticity is critical for a material to be used as an artificial vascular graft.[36] Thus a small-diameter vascular graft composed of fibroin and polyurethane was developed by electrospinning.[37] The parameters of electrospinning, particularly the target-syringe distance and collection time, were optimized to provide desired characteristics for vascular grafts. The target-syringe distance influenced the porosity of a graft and the collection time influenced its compressive elastic modulus and permeability. A fibroin/polyurethane graft was prepared by using the optimized parameters of a target-syringe distance of 9 cm and a collection time of 60 min. An electrospun graft with no fray on its cutting surface (Figure 6a) and exhibiting porosity but low permeability was successfully prepared. The graft was evaluated with a rat implantation test. A patency of 100% was obtained after implantation for 2 weeks ($n=2$) and 4 weeks ($n=4$). The formation of thrombus and intimal hyperplasia, which cause occlusion of the graft, was not observed. Moreover, as shown in Figure 6b, histological staining revealed that the organization of the blood vessel walls, which are composed of collagen, smooth muscle cells and endothelial cells, progressed on both sides of the graft surface. These results indicate that the biocompatibility of silk fibroin is conserved for fibroin/polyurethane complex grafts.

SUMMARY

The structures of silk fibroin before and after spinning were investigated by solution and solid-state NMR. For the fibroin structure before spinning, liquid silk extracted from silkworm larvae was measured, and sequential assignments of ^{1}H, ^{13}C and ^{15}N for repeat motifs were achieved. The molecular structures were determined for *B. mori* and *S. c. ricini* liquid silks. The precise lamellar structure of the repeat motif of *B. mori* fibroin after spinning was determined using a combination of a stable isotope labeling of peptides and solid-state NMR. In addition, a small diameter vascular graft was successfully developed by electrospinning, and the resulting graft exhibited high patency and engraftment. The results of these studies demonstrate that fibroin has good potential for use in novel processing techniques and biomedical materials.

CONFLICT OF INTEREST

The authors declare no conflict of interest.

ACKNOWLEDGEMENTS

I thank all my co-workers for their contributions and especially thank Professor Tetsuo Asakura, Professor Yasumoto Nakazawa (Tokyo University of Agriculture and Technology, Japan) and Professor Emeritus Heisaburo Shindo (Tokyo University of Pharmacy and Life Science) for their encouragement. Part of this work was supported by a Grant-in-Aid for Scientific Research (25810124).

1 Zhou, C. Z., Confalonieri, F., Jacquet, M., Perasso, R., Li, Z. G. & Janin, J. Silk fibroin: structural implications of a remarkable amino acid sequence. *Proteins Struct. Funct. Genet.* **44**, 119–122 (2001).
2 Yamaguchi, K., Kikuchi, Y., Takagi, T., Kikuchi, A., Oyama, F., Shimura, K. & Mizuno, S. Primary structure of the silk fibroin light chain determined by CDNA sequencing and peptide analysis. *J. Mol. Biol.* **210**, 127–139 (1989).
3 Inoue, S., Tanaka, K., Arisaka, F., Kimura, S., Ohtomo, K. & Mizuno, S. Silk fibroin of *Bombyx mori* is secreted, assembling a high molecular mass elementary unit consisting of H-chain, L-chain, and P25, with a 6: 6: 1 molar ratio. *J. Biol. Chem.* **275**, 40517–40528 (2000).
4 Tanaka, K., Kajiyama, N., Ishikura, K., Waga, S., Kikuchi, A., Ohtomo, K., Takagi, T. & Mizuno, S. Determination of the site of disulfide linkage between heavy and light chains of silk fibroin produced by Bombix mori. *Biochim. Biophys. Acta Protein Struct. Mol. Enzymol.* **1432**, 92–103 (1999).
5 Asakura, T., Ashida, J., Yamane, T., Kameda, T., Nakazawa, Y., Ohgo, K. & Komatsu, K. A repeated beta-turn structure in poly(Ala-Gly) as a model for silk I of *Bombyx mori* silk fibroin studied with two-dimensional spin-diffusion NMR under off magic angle spinning and rotational echo double resonance. *J. Mol. Biol.* **306**, 291–305 (2001).
6 Asakura, T., Yamane, T., Nakazawa, Y., Kameda, T. & Ando, K. Structure of *Bombyx mori* silk fibroin before spinning in solid state studied with wide angle x-ray scattering and C-13 cross-polarization/magic angle spinning NMR. *Biopolymers* **58**, 521–525 (2001).
7 Suzuki, Y., Yamazaki, T., Aoki, A., Shindo, H. & Asakura, T. NMR study of the structures of repeated sequences, GAGXGA (X=S, Y, V), in *Bombyx mori* liquid silk. *Biomacromolecules* **15**, 104–112 (2014).
8 Zhao, C. & Asakura, T. Structure of silk studied with NMR. *Prog. Nucl. Magn. Reson. Spectrosc.* **39**, 301–352 (2001).
9 Wishart, D. S., Sykes, B. D. & Richards, F. M. Relationship between nuclear-magnetic-resonance chemical-shift and protein secondary structure. *J. Mol. Biol.* **222**, 311–333 (1991).
10 Asakura, T., Iwadate, M., Demura, M. & Williamson, M. P. Structural analysis of silk with C-13 NMR chemical shift contour plots. *Int. J. Biol. Macromol.* **24**, 167–171 (1999).

11 Shen, Y. & Bax, A. Protein backbone and sidechain torsion angles predicted from NMR chemical shifts using artificial neural networks. *J. Biomol. NMR* **56**, 227–241 (2013).
12 Shen, Y. & Bax, A. Identification of helix capping and beta-turn motifs from NMR chemical shifts. *J. Biomol. NMR* **52**, 211–232 (2012).
13 Mai-ngam, K., Boonkitpattarakul, K., Jaipaew, J. & Mai-ngam, B. Evaluation of the properties of silk fibroin films from the non-mulberry silkworm *Samia cynthia ricini* for biomaterial design. *J. Biomater. Sci. Polym. Ed.* **22**, 2001–2022 (2011).
14 Kundu, S. C., Kundu, B., Talukdar, S., Bano, S., Nayak, S., Kundu, J., Mandal, B. B., Bhardwaj, N., Botlagunta, M., Dash, B. C., Acharya, C. & Ghosh, A. K. Invited review nonmulberry silk biopolymers. *Biopolymers* **97**, 455–467 (2012).
15 Kundu, B., Kurland, N. E., Bano, S., Patra, C., Engel, F. B., Yadavalli, V. K. & Kundu, S. C. Silk proteins for biomedical applications: bioengineering perspectives. *Prog. Polym. Sci.* **39**, 251–267 (2014).
16 Sezutsu, H. & Yukuhiro, K. The complete nucleotide sequence of the Eri-silkworm (*Samia cynthia ricini*) fibroin gene. *J. Insect Biotechnol. Sericol.* **83**, 59–70 (2014).
17 Xu, M. & Lewis, R. V. Structure of a protein superfiber: spider dragline silk. *Proc. Natl Acad. Sci. USA* **87**, 7120–7124 (1990).
18 Sponner, A., Schlott, B., Vollrath, F., Unger, E., Grosse, F. & Weisshart, K. Characterization of the protein components of *Nephila clavipes* dragline silk. *Biochemistry* **44**, 4727–4736 (2005).
19 Hinman, M. B. & Lewis, R. V. Isolation of a clone encoding a second dragline silk fibroin. *Nephila clavipes* dragline silk is a two-protein fiber. *J. Biol. Chem.* **267**, 19320–19324 (1992).
20 Suzuki, Y., Kawanishi, S., Yamazaki, T., Aoki, A., Saito, H. & Asakura, T. Structural determination of the tandem repeat motif in *Samia cynthia ricini* liquid silk by solution NMR. *Macromolecules* **48**, 6574–6579 (2015).
21 Marsh, R. E., Corey, R. B. & Pauling, L. An investigation of the structure of silk fibroin. *Biochim. Biophys. Acta* **16**, 1–34 (1955).
22 Fraser, R. D., MacRae, T. P. & Stewart, F. H. Poly-l-alanylglycyl-l-alanylglycyl-l-serylglycine: a model for the crystalline regions of silk fibroin. *J. Mol. Biol.* **19**, 580–582 (1966).
23 Lotz, B. & Cesari, F. C. Chemical-structure and the crystalline-structures of *Bombyx mori* silk fibroin. *Biochimie* **61**, 205–214 (1979).
24 Takahashi, Y., Gehoh, M. & Yuzuriha, K. Structure refinement and diffuse streak scattering of silk (*Bombyx mori*). *Int. J. Biol. Macromol.* **24**, 127–138 (1999).
25 Asakura, T., Sugino, R., Okumura, T. & Nakazawa, Y. The role of irregular unit, GAAS, on the secondary structure of *Bombyx mori* silk fibroin studied with C-13 CP/MAS NMR and wide-angle X-ray scattering. *Protein Sci.* **11**, 1873–1877 (2002).
26 Asakura, T., Yao, J., Yamane, T., Umemura, K. & Ulrich, A. S. Heterogeneous structure of silk fibers from *Bombyx mori* resolved by 13C solid-state NMR spectroscopy. *J. Am. Chem. Soc.* **124**, 8794–8795 (2002).
27 Suzuki, Y. & Asakura, T. Local conformation of serine residues in a silk model peptide, (Ala-Gly-Ser-Gly-Ala-Gly)(5), studied with solid-state NMR:REDOR. *Polym. J.* **42**, 354–356 (2010).
28 Suzuki, Y., Aoki, A., Nakazawa, Y., Knight, D. P. & Asakura, T. Structural analysis of the synthetic peptide (Ala-Gly-Ser-Gly-Ala-Gly)5, a model for the crystalline domain of *Bombyx mori* silk fibroin, studied with 13C CP/MAS NMR, REDOR, and statistical mechanical calcuations. *Macromolecules* **43**, 9434–9440 (2010).
29 Vepari, C. & Kaplan, D. L. Silk as a biomaterial. *Prog. Polym. Sci.* **32**, 991–1007 (2007).
30 Yao, J. M., Masuda, H., Zhao, C. H. & Asakura, T. Artificial spinning and characterization of silk fiber from *Bombyx mori* silk fibroin in hexafluoroacetone hydrate. *Macromolecules* **35**, 6–9 (2002).
31 Ha, S. W., Asakura, T. & Kishore, R. Distinctive influence of two hexafluoro solvents on the structural stabilization of *Bombyx mori* silk fibroin protein and its derived peptides: C-13 NMR and CD studies. *Biomacromolecules* **7**, 18–23 (2006).
32 Zhao, C. H., Yao, J. M., Masuda, H., Kishore, R. & Asakura, T. Structural characterization and artificial fiber formation of *Bombyx mori* silk fibroin in hexafluoro-iso-propanol solvent system. *Biopolymers* **69**, 253–259 (2003).
33 Trabbic, K. A. & Yager, P. Comparative structural characterization of naturally- and synthetically-spun fibers of *Bombyx mori* fibroin. *Macromolecules* **31**, 462–471 (1998).
34 Suzuki, Y., Gerig, I. T. & Asakura, T. NMR study of interactions between silk model peptide and fluorinated alcohols for preparation of regenerated silk fiber. *Macromolecules* **43**, 2364–2370 (2010).
35 Zhu, Z., Kikuchi, Y., Kojima, K., Tamura, T., Kuwabara, N., Nakamura, T. & Asakura, T. Mechanical properties of regenerated *Bombyx mori* silk fibers and recombinant silk fibers produced by transgenic silkworms. *J. Biomater. Sci. Polym. Ed.* **21**, 395–411 (2010).
36 Venkatraman, S., Boey, F. & Lao, L. L. Implanted cardiovascular polymers: natural, synthetic and bio-inspired. *Prog. Polym. Sci.* **33**, 853–874 (2008).
37 Suzuki, Y., Nakazawa, Y., Aytemiz, D., Komatsu, T., Miyazaki, K., Yamazaki, S. & Asakura, T. Development of silk/polyurethane small-diameter vascular graft by electrospinning. *Seikei Kakou* **25**, 181–187 (2013).

Yu Suzuki is a Senior Assistant Professor of Tenure-Track Program for Innovative Research at University of Fukui. She received her PhD from Tokyo University of Agriculture and Technology in 2010 under the supervision of Professor Tetsuo Asakura. After her research as an Assistant Professor, she joined the University of Fukui in 2014. She received the Award for Encouragement of Research in Polymer Science from the Society of Polymer Science, Japan in 2015. Her current research interests include NMR analysis of structure and dynamics of biopolymers.